Resonance enhanced multiphoton ionization of the hydrogen halides: Rotational structure and anomalies in Rydberg and ion-pair states of HCl and HBr

Ágúst Kvaran,[a] Huasheng Wang, and Áshildur Logadóttir
Science Institute, University of Iceland, Dunhaga 3, 107 Reykjavík, Iceland

(Received 22 November 1999; accepted 30 March 2000)

(2+1) resonance enhanced multiphoton ionization spectra have been recorded, simulated, and used to derive energies of rovibrational levels in the $F(^1\Delta)$, $E(^1\Sigma^+)$, and $V(^1\Sigma^+)$ states for HCl ($H^{35}Cl$ and $H^{37}Cl$) and HBr ($H^{79}Br$ and $H^{81}Br$). Spectroscopic parameters derived for the *F* states compare nicely with those derived by others using conventional analysis methods. Clear evidence for *near resonance* interactions between the *F* and the *V* states is seen for the first time, both in HCl and HBr. Shape of curves for rotational level energy spacings versus rotational quantum numbers are found to depend characteristically on the nature of *off-resonance* interactions observed between the *E* and the *V* states. Model calculations for state interactions, based on perturbation theory, are performed for HCl. These prove to be useful to interpret observed perturbations, both qualitatively and quantitatively. Interaction strengths are evaluated for *F* to *V* and *E* to *V* state interactions. Variations observed in the intensity ratios of *O* and *S* line series to *Q* line series in vibrational bands of the *V* state for HCl are discussed and mechanisms of two-photon excitation processes are proposed.
 [S0021-9606(00)01824-9]

I. INTRODUCTION

Low resolution vacuum ultraviaolet absorption spectra of the hydrogen halides were first reported and studied in 1938 by Price.[1] Since then a wealth of spectroscopic data has been derived from high resolution absorption spectroscopy,[2–12] fluorescence studies,[12,13] as well as from resonance enhanced multiphoton ionization (REMPI) experiments[14–27] on HCl,[4–6,12,14–20,22,23,26,27] DCl,[4,5] HBr,[2,3,9,13,21–23,27] DBr,[9] HI,[7,8,11,22–25,27] and DI.[7,8,10] Large numbers of Rydberg states have been identified by means of absorption spectroscopy[2–13] and weak absorption is observed due to transitions to the $V(^1\Sigma^+)$ ion-pair states.[5,8–12] Fluorescence spectroscopy has been found to be more useful to characterize the $V(^1\Sigma^+)$ ion-pair state,[12,13] while only a weak fluorescence is observed from the Rydberg states. This latter behavior is attributed to a strong predissociation.[12] REMPI spectroscopy has proved to be a very successful technique for rotational structure analysis of all these Rydberg and valence states[23] as well as for identifying new states which are not observed by conventional single photon spectroscopic methods.[28] A number of spin-nonallowed transitions are observed, indicating that spin–orbit coupling is important in these molecules.[12] Theoretical *ab initio* calculations on the electronic states of HCl have been found to be capable of verifying qualitatively and, in some instances, quantitatively all the bands in the HCl spectrum observed.[29]

Perturbations due to state mixing are widely seen both in absorption[3,5–8,10–13] and REMPI spectra[15,16,18,20,21,23,24,27] of HCl,[5,6,12,15,16,18,20,23,27] DCl,[5] HBR,[3,13,21,23,27] HI,[7,8,11,24,27] and DI.[7,8,10] The perturbations appear either as line shifts[6,15,16,18,23,27] or as intensity and/or bandwidth alterations.[6,15,16,18,20,23] Pronounced ion-pair to Rydberg state mixings are observed in the $^{3,1}\Sigma^+$ manifolds both experimentally[5,6,16,18,20,21,23,27] and theoretically.[29] Interactions between the $V(^1\Sigma^+)$ ion-pair states and the $E(^1\Sigma^+)$ states are found to be particularly strong. It has been shown that the interaction causes a characteristic compression of rovibrational levels in the *E* state manifold but an expansion of levels in the *V* state manifold.[27] Comparable perturbative effects, on the other hand, have been *predicted* not to occur for their counterparts of Π, Δ, and Σ^- symmetry.[29] Nevertheless, perturbations have been observed in such Rydberg systems,[6,20,21] which, guided by the theoretical predictions,[29] have been interpreted to be due to Rydberg–Rydberg mixings.[20,21] While most perturbation effects observed are believed to be homogeneous in nature ($\Delta\Omega=0$),[27,29] heterogeneous ($\Delta\Omega=\pm1$) couplings have been proposed to occur in the $F^1\Delta$ state for HCl.[20]

Numerous reasons exist for spectroscopic studies of the hydrogen halides. In addition to a pure interest in molecular spectroscopy, quantitative data on the hydrogen halides are of interest to understand stratospheric photochemistry.[12,13] Furthermore, such data are relevant to the photochemistry of planetary atmospheres and the interstellar medium.[12,13] Last but not least detailed studies of REMPI spectra of small molecules, such as the hydrogen halides, are of importance to determine relative populations of quantum states in conjunction with a frequent use of REMPI detection of product molecules in reaction dynamics.[20,30,31]

In this paper we present studies of (2+1) REMPI rotational spectra of HCl and HBr, emphasizing analysis of the rotational energy structures of various vibrational states of

[a]Electronic mail: agust@raunvis.hi.is

the $F(^1\Delta)$, $E(^1\Sigma^+)$, and the $V(^1\Sigma^+)$ states. Experimental spectra, recorded at room temperature, are compared with calculated (simulated) spectra, obtained for unperturbed systems and/or used to derive energies and energy spacings of rotational quantum levels in the excited states. Spectroscopic parameters for the F states are obtained and data are interpreted and analyzed in order to derive both qualitative and quantitative information on state interactions. All major perturbation effects observed can be understood as arising from Rydberg to ion-pair interactions and evidence for $F(^1\Delta)$ to $V(^1\Sigma^+)$ near resonance interactions is presented for the first time. Model calculations, based on perturbation theory, are performed to simulate both E to V and F to V state interactions observed. Furthermore, information on the resonance excitation processes is derived.

II. EXPERIMENTS AND METHODS OF ANALYSIS

A. Experiments

The apparatus used has been described in detail elsewhere[23,32,33] so only a brief report will be given here. Tunable radiation was generated by an excimer laser-pumped dye laser system from Lumonics. For wavelengths less than about 330 nm, the laser output was frequency doubled by suitable SHG crystals. The frequency-doubled beam was separated from the fundamental by a Pellin Broca prism. The radiation was focused into an ionization cell between two electrodes. The cell contained gas samples at low pressure. Current pulses in the gas due to laser pulse photoionization caused voltage drops across the electrodes. After amplification and integration the voltage pulses were fed into a multichannel analyzer for peak height measurements and recording. Finally, average pulse heights for a fixed sampling time were recorded to get the spectrum. Typically spectral points were obtained by averaging over 100 pulses. The bandwidth of the dye laser beam was about 0.05 cm^{-1}. Care was taken to prevent power broadening due to ac Stark effects by minimizing laser power. Wavelength calibration was achieved either by recording neon or iodine atomic lines[34] or by comparison of the strongest hydrogen chloride rotational lines with those reported by Green, Bickel, and Wallace.[17] The accuracy of the calibration, as judged from the position of the atomic lines, was found to be ± 2 cm^{-1} on the two-photon wavenumber scale.

B. Spectra analysis

1. Spectra simulations

Details of our procedure for calculating two-photon absorption spectra to represent (2+1) REMPI spectra have been given elsewhere.[27,33,35] The spectra calculations require evaluations of *line positions* and *line strengths.*

Line positions for rovibrational lines can be expressed as

$$\nu_{J',v'\leftarrow J'',v''}=\nu^0_{v',v''}+\Delta E_{J',J''}, \tag{1}$$

where $\nu^0_{v',v''}$ is the band origin of a vibrational band, depending on the vibrational parameters $(\omega_e,\omega_e x_e)$ and the vibrational quantum numbers (v',v'') for the two electronic states. $\Delta E_{J',J''}$ is the difference in rotational energies, depending on the rotational parameters (B,D) and the rotational quantum numbers (J',J'') for the two states.

The relative rotational *line intensities* $(I_{\rm rel})$ for a vibrational band are proportional to a product of the Boltzmann population and the ''two-photon absorption strength'' $(S_{v'v''})$ as determined by Bray and Hochstrasser,[36]

$$I_{\rm rel}=CS_{v'v''}\exp(-E(J'')/kT). \tag{2}$$

Finally, rotational lines were displayed as *Gaussian-shaped functions* using bandwidths which gave the best fits of calculated and experimental line profiles.

The simulation procedure involved either least-squares analysis in terms of positions of rotational lines or visual comparison of calculated and experimental spectra. In cases when clear displacements of rotational lines due to near-resonance state interactions were observed (see the following) only seemingly nondisplaced rotational lines were taken into account in the simulation procedure. Thus a comparison between unperturbed (calculated) and perturbed (experimental) spectra was sought. The analysis allowed estimates of rotational parameters for the upper states.

2. Rovibrational energies

Energies of rovibrational levels in the excited state, relative to the minimum electronic energy of the molecule in the ground state (T''_e) (i.e., $E_{v',J'}$), were evaluated from those in the ground electronic state for the lowest vibrational quantum number, $v''=0$ $(E_{v''=0,J''})$, and from measured wavenumbers for the corresponding transition $(\nu_{v',J'\leftarrow v''=0,J''})$ for the isotopomers $H^{35}Cl$ and $H^{81}Br$,

$$E_{v',J'}=\nu_{v',J'\leftarrow v''=0,J''}+E_{v''=0,J''}, \tag{3}$$

where

$$E_{v''=0,J''}=1/2\omega''_e-1/4\omega_e x''_e+B_{v''=0}J''(J''+1/2)-D_{v''=0}J''^2(J''+1/2)^2, \tag{4}$$

$$B_{v''=0}=B''_e-1/2\alpha''_e, \tag{5}$$

$$D_{v''=0}=4(B_{v''=0})^3/\omega''^2_e \tag{6}$$

for known ground state vibrational $(\omega''_e,\omega_e x''_e)$ and rotational (B''_e,α''_e) parameters.[27,37] Finally, rotational energy differences for the excited states $(\Delta E_{J'+1,J'})$

$$\Delta E_{J'+1,J'}=E_{v',J'+1}-E_{v',J'} \tag{7}$$

plotted as a function of $E_{v',J'}$ or J' were found to be useful for detailed inspections of the rotational energy structures.

III. RESULTS AND INTERPRETATIONS

A. Spectra simulations

Rotational parameters, derived from simulations of the $E\leftarrow X$ and the $V\leftarrow X$ spectra, have already been published.[27] Due to severe perturbations in these systems, however, good quality fits were often difficult to obtain. Hence, the parameters derived cannot be accepted as being representative values for unperturbed states and a more detailed analysis of the rotational energy structure needs to be undertaken (see the following). Rotational parameters for the $F(^1\Delta)$ states per

TABLE I. Vibrational (band origins and spacings between v' levels) and rotational parameters for the $F(^1\Delta)$ states of $H^{35}Cl$ and $H^{81}Br$.

Compound	v'	ν^0		$\Delta\nu^0(v',v'-1)$	$B'(\mathrm{cm}^{-1})$		$D'\times10^3(\mathrm{cm}^{-1})$		References for others' work
		Our work	Others' work	Our work	Our work	Others' work	Our work	Other's work	
$H^{35}Cl$	0	82 849.3	82 847.2(A')		10.295(A')	10.3246(A')	1.01(A')	0.9837(A')	17
			82 847.4(A'')		10.314(A'')	10.3228(A'')	1.25(A'')	1.0925(A'')	
$H^{35}Cl$	1	85 358.9	85 363.7(A')	2509.6	10.133(A')	10.143(A')	1.62(A')	1.0659(A')	17
			85 363.8(A'')		10.153(A'')	10.1447(A'')	2.12(A'')	1.7346(A'')	
$H^{35}Cl$	2	87 769.8	87 772.4(A')	2410.9	10.2578(A')	10.256(A')	5.15(A')	5.153(A')	17
			87 772.4(A'')		10.2578(A'')	10.248(A'')	3.15(A'')	5.004(A'')	
$H^{81}Br$	0	77 012.3	77 009.3		8.2027(A')	8.202(A')	0.38(A')	0.4(A')	21
					8.2028(A'')	8.25(A'')	0.26(A'')	6.6(A'')	
$H^{81}Br$	1	79 305.5	79 306.0	2293.2	7.976(A')	7.998(A')	0.51(A')	0.7(A')	21
					7.980(A'')	7.904(A'')	0.30(A'')	−0.3(A'')	

vibrational states, as well as band origins derived from the simulations procedure, are summarized in Table I along with values derived by others. Generally our values compare nicely with those derived by Green, Bickel, and Wallace for HCl[17] and Callaghan and Gordon for HBr,[21] who both used conventional rotational analysis methods. Table II shows derived spectroscopic parameters, characteristic for the electronic states ($F(^1\Delta)$). Apart from small localized line shifts (see the following), the spectra of the $F\leftarrow X$ transitions were found to be less perturbed and easier to simulate. Hence, there is a reason to believe that the derived spectroscopic parameters (Tables I and II) are good representatives for unperturbed F states. In Fig. 1 vibrational energy levels for the F, E, and V states, as well as the rotational constants for the V states, are plotted for $H^{35}Cl$ and $H^{81}Br$.

Figure 2 shows experimental and calculated spectra for the Q branches of the $(v'=1,v''=0)$ bands of the $F(^1\Delta)\leftarrow X(^1\Sigma)$ electronic transitions for HCl and HBr. Small but significant shifts (compression) of rotational lines, relative to those calculated, are found in both cases, for $J'=7$ and 8 in HCl (both $H^{35}Cl$ and $H^{37}Cl$) and for $J'=5$ and 6 in HBr. Lines for $J'=7$ in HCl and $J'=5$ in HBr shift to the red while lines for $J'=8$ in HCl and $J'=6$ in HBr shift to the blue with respect to the calculated lines. This suggests that the corresponding rotational energy levels, $J'=7$ in HCl and $J'=5$ in HBr, shift up in energy, while levels $J'=8$ in HCl and $J'=6$ in HBr shift down. In both cases the shifts are found to be larger for the higher J' numbered lines/levels. Furthermore, intensity irregularities are observed in the vicinity of these lines, as seen by comparing the calculated and experimental spectra. First, the shifted line intensities deviate from a regular intensity pattern in the Q series by showing larger intensities for the higher numbered lines. Second, the observed line intensities fall off less rapidly with J quantum numbers than predicted.

B. Rovibrational energies

Figure 3 shows rovibrational levels for the $F(^1\Delta)$, $E(^1\Sigma^+)$, and the $V(^1\Sigma^+)$ states, $v'=0$ and 1 for the F and the E states and $v'=9-15$ for the V state of $H^{35}Cl$. Spacings $(\Delta E_{J'+1,J'})$ of neighboring energy levels, derived from the various rotational line series, are shown to the right in Figs. 3(b) and 3(c) (dotted lines and markers) plotted as a function of $E_{v'J'}$ [more precisely as a function of $E_{v'J'}+(\Delta E_{J'+1,J'})/2$] tilted by 90°. Corresponding curves for unperturbed rotational levels/rigid rotor $[E_{J'}=B'J'(J'+1)]$ for $B'=3\ \mathrm{cm}^{-1}$ $(D'=0)$ are also shown (solid curves) as reference curves. Figures 4 and 5 show spacing values $(\Delta E_{J'+1,J'})$ plotted as a function of J' (more precisely as a function of $J'+1/2$) along with reference curves for selected vibrational states in HCl and HBr, respectively. Notice that in this case the reference curves are linear functions $[(\Delta E_{J'+1,J'})=2B'J']$. In general, good agreement is found between $E_{v',J'}$ values (hence between $\Delta E_{J'+1,J'}$ values) derived from different rotational line series within the same vibrational band (see Figs. 3–5).

Generally, the overall spacing between rotational energy levels, within a vibrational state in the V state, is found to increase as the vibrational states get closer to those in the E state (an expansion of levels). Thus, the energy level expansion changes as $(v'_V=10)>(v'_V=11)\gg(v'_V=9)$ as seen in Fig. 3(b) and as $(v'_V=14)>(v'_V=13)$ as seen in Fig. 3(c) for HCl. This is an effect of the E to V state interaction, which, according to a standard perturbation theory,[38,39] can be viewed as involving level-to-level repulsion between states with the same J quantum numbers. Such an interaction will be inversely dependent on vibrational level separations.[38] The overall effect, in a situation like the present, will be an expansion of levels in the ion-pair state (V state) and compression of levels in the Rydberg state (E state). Such inter-

TABLE II. Vibrational and rotational spectroscopic parameters and average internuclear distances for the $F(^1\Delta)$ states of $H^{35}Cl$ and $H^{81}Br$ derived from our data in Table I.

Compounds	$T'_e(\mathrm{cm}^{-1})$	$\omega'_e(\mathrm{cm}^{-1})$	$\omega_e x'_e(\mathrm{cm}^{-1})$	$B'_e(\mathrm{cm}^{-1})$	$\alpha'_e(\mathrm{cm}^{-1})$	$D'_e\times10^3$ (cm^{-1})	r_e(Å)
$H^{35}Cl(A')$	83 040	2608.3	49.35	10.256	0.0186	0.643	1.295
$H^{81}Br(A')$	77 179	2293.2	?	8.316	0.226	0.437	1.426

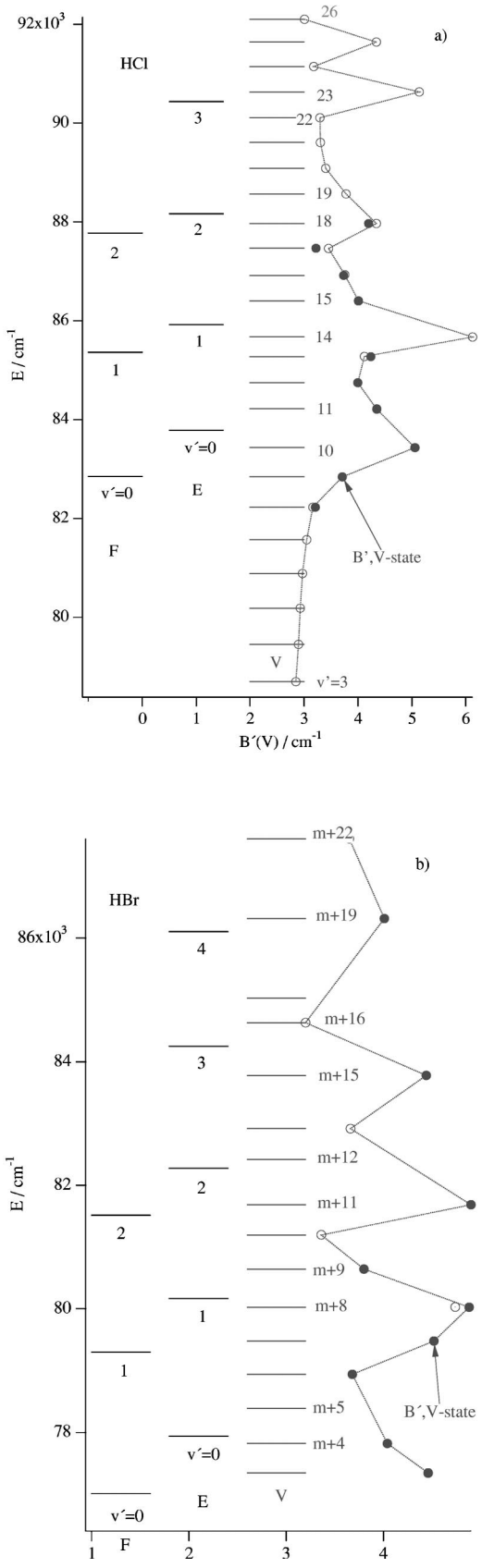

FIG. 1. Vibrational energy levels for F, E, and V states and rotational constants (B') for the V states plotted as a function of energy for (a) HCl and (b) HBr. Closed circles: our work, open circles: others' work (Refs. 15 and 21).

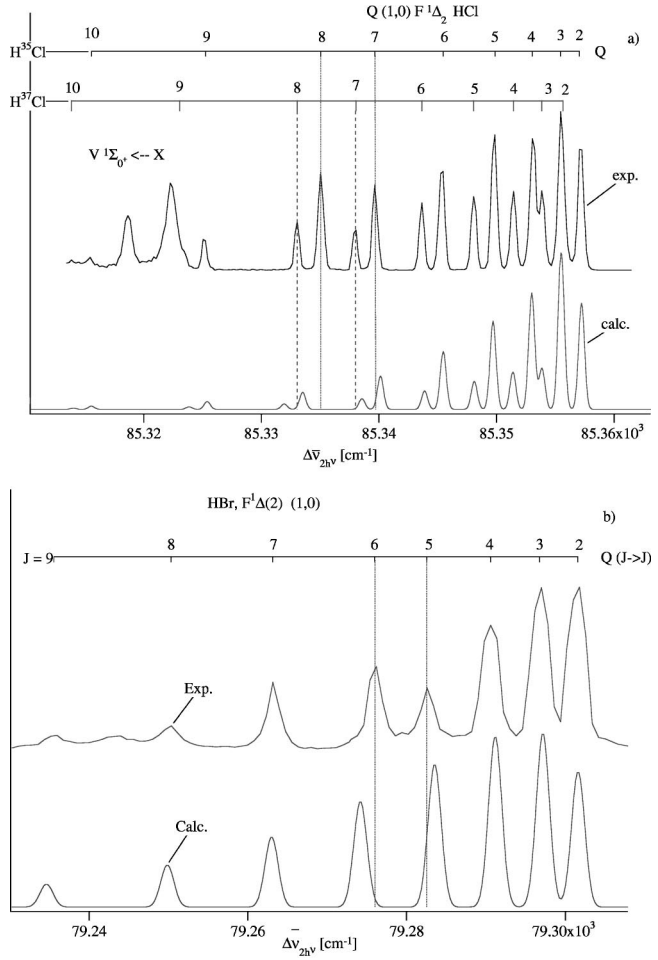

FIG. 2. Simulations of Q line series in (2+1) REMPI, (1,0) vibrational bands of the $F(^1\Delta)\leftarrow X$ spectra for (a) HCl ($H^{35}Cl$ and $H^{37}Cl$) and (b) HBr. Rotational lines, which are found to be shifted with respect to calculated line positions, are indicated by dashed lines (see the text).

actions are shown schematically in Fig. 4 of Ref. 27 in terms of rotational-to-rotational interactions, while in Fig. 3(a) of the present article they are represented schematically in terms of overall interactions between rovibrational states.

C. Interpretations: Spectra and level spacings

1. F vs V interactions

The following observations concerning the F and the V states for HCl and HBr suggest that a *near-resonance* interaction is occurring between the two states.

a. HCl, $F(v'=1)\leftrightarrow V(v'=14)$. The observed increase in separation of rotational levels $J'=7$ and 8 in the F state, $v'=1$ [Fig. 2(a)], also weakly seen in the $\Delta E_{J'+1,J'}$ vs $E_{v'J'}$ plot in Fig. 3(c), coincides with an observed decrease in spacing between levels with the same J quantum numbers in the V states, $v'=14$, as seen in Figs. 3(c) and 4(c). A smaller energy difference between the two $J=8$ levels than between the two $J=7$ levels [Fig. 3(c)] explains why a larger shift is observed for the $J'=8$ rotational Q line [Fig. 2(a)].

b. HBr, $F(v'=1)\leftrightarrow V(v'=m+7)$. The observed increase in separation of rotational levels $J'=5$ and 6 in the F state, $v'=1$ [Fig. 2(b)], coincides with an observed decrease in spacing between near-resonance levels with the same J quan-

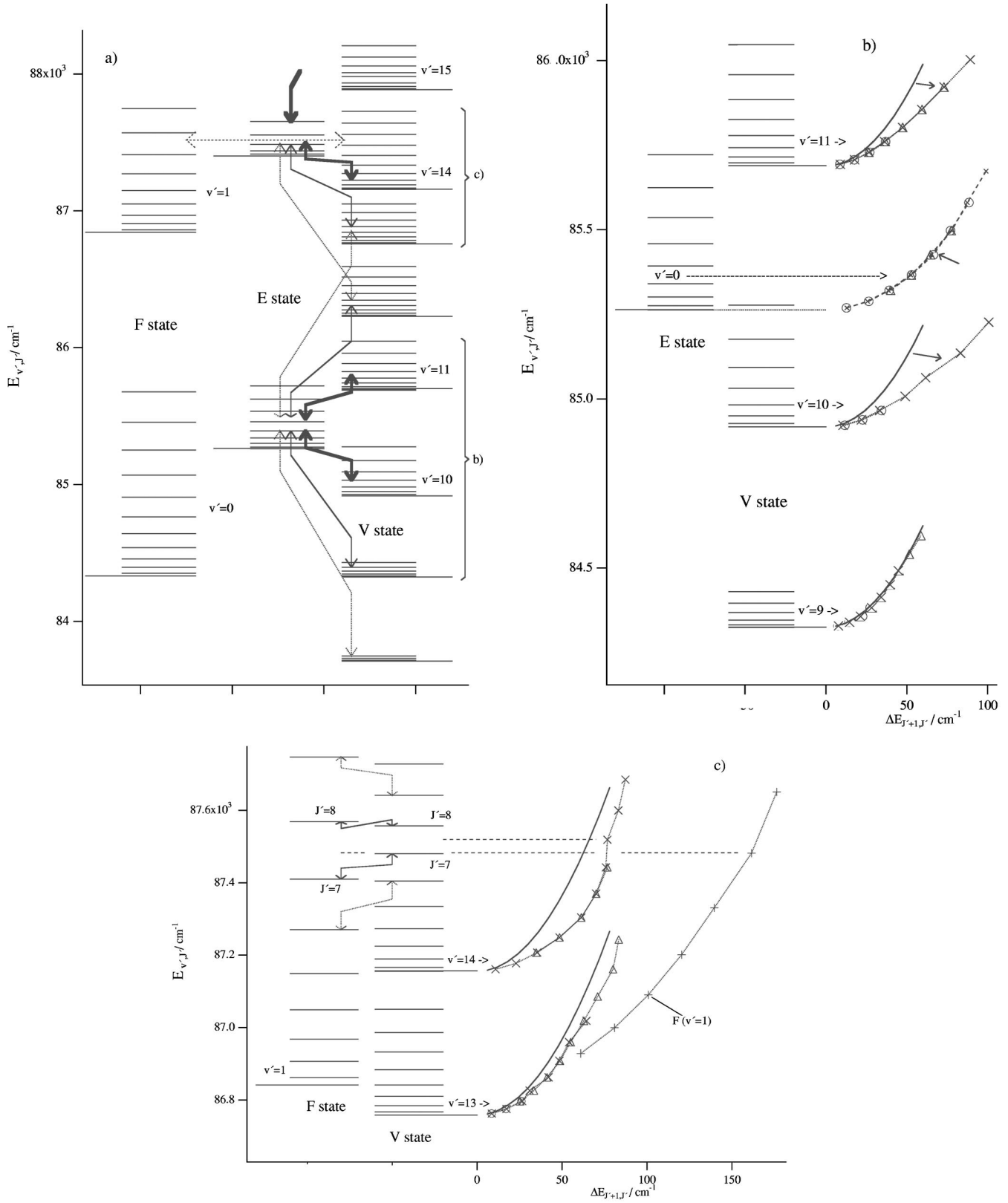

FIG. 3. $H^{35}Cl$: Rovibrational levels for the $F(^1\Delta)$, $E(^1\Sigma^+)$, and the $V(^1\Sigma^+)$ states. (a) F, $E(v'=0,1)$ and $V(v'=8-5)$: Strength and direction of *off-resonance* repulsive type interactions between rovibrational states within the E and the V states are indicated by arrows. Increasing broadness of arrows refers to larger interaction strengths. *Near-resonance* interaction regions observed between the F and the V states are indicated by a vertical dashed arrow. (b) $E(v'=0)$ and $V(v'=9-11)$—effect of *off-resonance interaction*: Spacings between neighbor rotational levels, derived from different rotational line series (dashed lines and markers; O:○, Q:× and S:△) along with reference curves (solid lines) for $B'=3$ cm^{-1} are plotted to the right. Arrows indicate effects of state interactions on energy spacings. (c) $F(v'=1)$ and $V(v'=13,14)$—effect of *near-resonance interaction*: Spacings between levels presented as in (b). Effects of interactions on level spacing are indicated. The arrows show $F \leftrightarrow V$ interaction strengths and directions. Dashed lines indicate what level spacings are affected by the interaction.

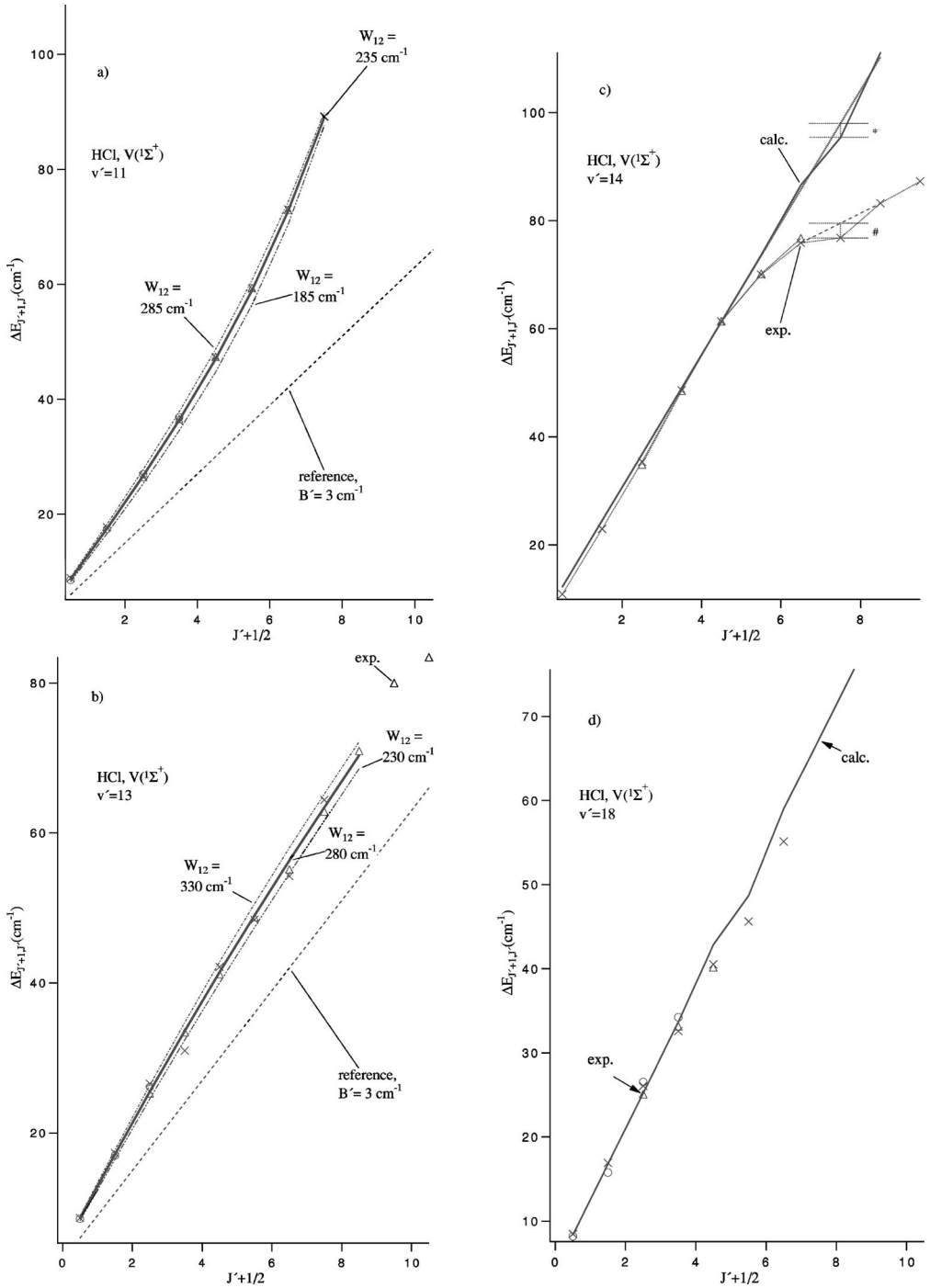

FIG. 4. HCl, state interaction effects: Spacings between V state rotational levels vs $J'+1/2$, derived from different rotational line series markers; O:○, Q:× and S:△) and calculated curves based on state interactions. Different calculated curves are shown in (a) and (b) to demonstrate the precision of the fitting procedure. Reference curves for $B'=3$ cm^{-1} serve the purpose to guide the eye. (a) $E(v'=0)\leftrightarrow V(v'=11)$ interaction: Input parameters for the perturbation calculation were as follows: $\Delta E^0_{v'}=+380$ cm^{-1}, $B^0(V)=3.397$ cm^{-1}, $B^0(E)=8.37$ cm^{-1}. W_{12} values for the calculated curves are indicated. Best fit was obtained for $W_{12}=235$ cm^{-1}. (b) $E(v'=1)\leftrightarrow V(v'=13)$ interaction: Input parameters for the perturbation calculation were as follows: $\Delta E^0_{v'}=-520$ cm^{-1}, $B^0(V)=3.55$ cm^{-1}, $B^0(E)=8.37$ cm^{-1}. W_{12} values for the calculated curves are indicated. Best fit was obtained for $W_{12}=280$ cm^{-1}. (c) $F(v'=1)\leftrightarrow V(v'=14)$ interaction: Input parameters for the perturbation calculation were as follows: $\Delta E^0_{v'}=+250$ cm^{-1}, $B^0(V)=6.126$ cm^{-1}, $B^0(F)=10.10$ cm^{-1}, $W_{12}=0.82(J(J+1))^{1/2}$ cm^{-1}. The straight line refers to the zero-order level spacing without $F\leftrightarrow V$ interaction. Drops in spacings due to interaction are marked with an asterisk (experimental) and a sharp sign (calculated). (d) $F(v'=2)\leftrightarrow V(v'=18)$ interaction: Input parameters for the perturbation calculation were as follows: $\Delta E^0_{v'}=+195$ cm^{-1}, $B^0(V)=4.198$ cm^{-1}, $B^0(F)=10.25$ cm^{-1}, $W_{12}=0.86(J(J+1))^{1/2}$ cm^{-1}.

tum numbers in the V states, $v'=m+7$ [Fig. 5(a)]. This is a situation comparable to that described previously for HCl. Comparison of rotational level energies reveals less energy difference between the $J=6$ levels than between the $J=5$ levels, which explains why a larger shift is observed for the $J'=6$ rotational Q line [Fig. 2(b)].

c. HCl, F(v′=2)↔V(v′=18). A slight but significant decrease in the spacing between $J'=5$ and 6 levels is ob-

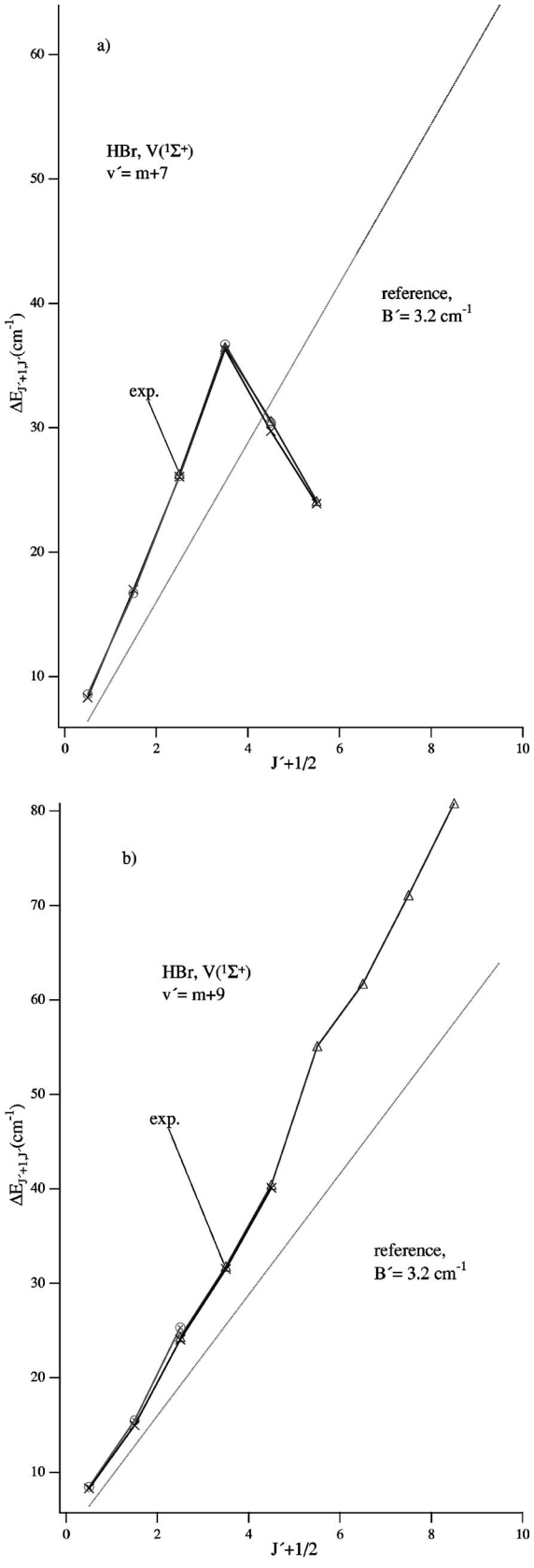

FIG. 5. HBr, state interaction effects: Spacings between V state rotational levels vs $J'+1/2$, derived from different rotational line series (lines and markers; O:○, Q:× and S:△) along with reference curves (solid straight lines) for $B'=3.2$ cm^{-1}, showing (a) dominant effect of $F(v'=1)\leftrightarrow V(v'=m+7)$ *near-resonance* interaction, (b) dominant effect of $E(v'=0)\leftrightarrow V(v'=m+9)$ *off-resonance* interaction.

served in the V state, $v'=18$ [Fig. 4(d)], which can be explained as being due to effects of near-resonance levels with the same quantum numbers in the F state, $v'=2$. Again this is a situation comparable to that described previously.

2. E vs V interactions

Either positive or negative curvatures are observed in plots of $\Delta E_{J'+1,J'}$ vs J' for those vibrational states within the V state which are close in energy to vibrational states within the E state [Figs. 4(a), 4(b), and 5(b)]. Similar observations, although less clear, have been found for the E states. This is a result of *off-resonance* level interactions characteristic of these states, as will be demonstrated in the following.

3. Model calculations for HCl

The above-mentioned observations, due both to the *near-resonance* and *off-resonance* interactions, were tested against a calculation model for state interactions based on perturbation theory. Level to level interactions are represented by

$$E=(1/2)(E_1^0+E_2^0)\pm(1/2)[4|W_{12}|^2+(E_1^0-E_2^0)^2]^{1/2}, \quad (8)$$

where E_1^0 and E_2^0 are the zero-order rovibrational level energies for states 1 and 2 and W_{12} is the matrix element of the perturbation function/the interaction strength. The E's are the resulting level energies. In the case of $F\leftrightarrow V$ interactions an attempt was made to image the observed dips in the $\Delta E_{J'+1,J'}$ vs J' curves for the V state, while in the cases of $E\leftrightarrow V$ interactions the curvature of the $\Delta E_{J'+1,J'}$ vs J' plots for the V state was sought. In the case of the *off-resonance* interactions ($E\leftrightarrow V$) emphasis was placed on interpreting structures where there was reason to believe that the major interactions were associated with two vibrational states, i.e., cases of vibrational states close in energy. It should be emphasized that zero-order energies cannot be determined precisely, since each vibrational state will be affected by more than one perturbing vibrational state [see Fig. 3(a)], while in the model calculation only interactions between two sets of rovibrational states are assumed. Zero-order energies were chosen to fulfill the following criteria.

(1) Zero-order energy differences between the *vibrational* states ($J'=0$) of the V state and the Rydberg state (F or E), $\Delta E_{v'}^0=E_{v'}^0(V)-E_{v'}^0(\mathrm{Ry})$, were chosen to be comparable or slightly less than the observed differences ($\Delta E_{v'}$) and to fulfill the following requirements. (a) All zero-order energy levels of the Rydberg state are either higher or lower in energy than those for the V state in the cases of *off-resonance* interactions ($E\leftrightarrow V$ interactions). (b) Zero-order energy levels of *near-resonance* interacting rotational states ($F\leftrightarrow V$)($E_{J'+1}^0(V)\leftrightarrow E_{J'+1}^0(F)$ and $E_{J'}^0(V)\leftrightarrow E_{J'}^0(F)$) fulfill the requirement: $E_{J'+1}^0(V)<E_{J'+1}^0(F)$, $E_{J'}^0(V)>E_{J'}^0(F)$.

(2) Zero order *rotational* energies within each vibrational state ($E_{J'}^0$) were represented by

$$E_{J'}^0(V)=B^0(V)J'(J'+1), \quad (9)$$

$$E_{J'}^0(\mathrm{Ry})=B^0(\mathrm{Ry})J'(J'+1), \quad (10)$$

where $B^0(V)$ and $B^0(\mathrm{Ry})$ are the zero-order rotational constants for the two states. The largest perturbation effects are due to the *off-resonance* interaction. Hence the deperturbed values derived by Liyanage, Gordon, and Field were used in the analysis of the $E-V$ interaction,[40] but the effective rotational constants, derived directly from the spectra[27] were used in the analysis of the *near-resonance* $F-V$ interaction. (a) The deperturbed rotational constant values for the V state are lower than or equal to the corresponding observed value, because of the *expansion* in rotational levels within the V state due to the $E-V$ interaction. (b) The deperturbed rotational constant values for the V state are larger than or equal to the corresponding observed value, because of the *compression* in rotational levels within the Rydberg state due to the $E-V$ interaction.

The $E(^1\Sigma^+)$ to $V(^1\Sigma^+)$ perturbation is clearly due to a *homogeneous* coupling ($\Delta\Omega=0;\Omega=0$). By definition the $F(^1\Delta)$ state is an $\Omega=2$ state. However, it has been pointed out that $F(^1\Delta)$ most likely is a mixed state.[20] First, the observation of the F state in the one-photon spectrum implies that the wave function contains some $\Omega<2$ character. Second, spin–orbit coupling is found to mix the $F(^1\Delta_2)$ and the $f(^3\Delta_2)$ states. Therefore the $F(^1\Delta)$ state wave function may in fact be a linear combination of $\Omega=1,2$, and 3 components in which case the weak perturbation observed most likely is due to a *heterogeneous* ($\Delta\Omega=1$) coupling. Accordingly, W_{12} was treated as a constant for the $E-V$/*homogeneous* interaction, but assumed to be proportional to the square root of $J(J+1)$ for the $F-V$/*heterogeneous* interaction,[39] i.e.,

$$W_{12}=W'_{12}(J(J+1))^{1/2}. \tag{11}$$

The fitting procedure involved adjusting two parameters only, W_{12} (or W'_{12}) and $\Delta E^0_{v'}$, for restricted values of $\Delta E^0_{v'}$. Figure 4 shows the results of model calculations for interactions between sets of rovibrational levels for (a) medium interaction strengths, relevant to $E\leftrightarrow V$ interactions [Figs. 4(a) and 4(b)] and (b) low interaction strengths, relevant to $F\leftrightarrow V$ interactions [Figs. 4(c) and 4(d)], obtained for HCl. Parameters used in these curve structure analyses are given in the figure captions.

The following *qualitative* conclusions can be obtained from this analysis. First, the characteristic curvatures in the $\Delta E_{J'+1,J'}$ vs J' graphs for the V state could be reproduced [Figs. 4(a) and 4(b)]. A positive curvature [Fig. 4(a)] is obtained for an interaction where the (major) perturbing Rydberg state (here: $v'=0,E$ state) is lower in energy than the perturbed state (here: $v'=11,V$ state), i.e., $\Delta E^0_{v'}>0$ (here: $+380\ \mathrm{cm}^{-1}$). A negative curvature [Fig. 4(b)], on the other hand, is observed for $\Delta E^0_{v'}<0$ (here: $-520\ \mathrm{cm}^{-1}$ for interaction between $v'=1$ in F and $v'=13$ in V). Second, ''localized'' dips in $\Delta E_{J'+1,J'}$ vs J' curves were reproduced in the cases of near-resonance interaction [Figs. 4(c) and 4(d)]. The characteristic curvature, observed in the $\Delta E_{J'+1,J'}$ vs J' plots for those v'_V states close in energy to vibrational states of the E state, was not found for vibrational levels mid between E-state levels (such as $v'_V=12$, 16, and 20), or for the v'_E states. Most probably this is due to a simultaneous downfield and upfield shifts by adjacent rovibrational states of the perturbing state, resulting in near canceling of shift effects.

Trial and error fitting analysis of the $\Delta E_{J'+1,J'}$ vs J' graphs allowed estimates of transition strengths. Uncertainty in the zero-order energy differences limited its certainty, however [see Figs. 4(a) and 4(b)]. Thus we conclude that the $E\leftrightarrow V$ interaction strength in the vicinity of the $v'=0$ state of the E state is of the order $235\pm100\ \mathrm{cm}^{-1}$, but that the $E\leftrightarrow V$ interaction strength near $v'=1$ in the E state is of the order $280\pm100\ \mathrm{cm}^{-1}$. These rather large perturbation matrix elements cause significant shifts of the vibrational energies. Thus the vibrational states $v'_E=0$ and $v'_V=11$ [Fig. 4(a)], on the one hand, and the $v'_E=1$ and $v'_V=13$ [Fig. 4(b)], on the other hand, are found to be pushed apart by about 220 and $240\ \mathrm{cm}^{-1}$, respectively. This corresponds to an upfield shift of about $110\ \mathrm{cm}^{-1}$ for $v'_V=11$ and downfield shift of about $120\ \mathrm{cm}^{-1}$ for $v'_V=13$. This effect is clearly seen by large alterations in vibrational level spacings in the V state as demonstrated in Ref. 27, Fig. 3 [see also Fig. 1(a) here]. Thus the spacing between $v'_V=13$ and 14 is $398\ \mathrm{cm}^{-1}$ but is $728\ \mathrm{cm}^{-1}$ between $v'_V=14$ and 15, compared to the average value of about $570\ \mathrm{cm}^{-1}$ between $v'_V=8-19$.[27] Analysis of the interaction between $v'_E=1$ and $v'_V=14$ [see Figs. 3(c) and 4(c)] revealed downfield shift of the $v'_V=14$ level by about 270 cm^{-1} and resulted in spacing value close to that observed between $v'_V=13$ and 14. The interaction strength was found to decrease as v' of the E state increased further. The matrix element of the perturbing function, W_{12}, can be assumed to be proportional to the overlap integral of the vibrational wave functions involved in a first approximation.[38] Hence, these results suggest that the crossing point of the two states is at an energy close to that between $v'=0$ and $v'=1$ for the E state, as has been suggested before.[27]

Comparison of the calculated and observed dips in the $\Delta E_{J'+1,J'}$ vs J' curves for $v'=14$ and 18 for the V state reveals interaction strengths between the F and the V states which vary with J as $W'_{12}(J(J+1))^{1/2}$ for $W'_{12}\sim0.8-0.9\ \mathrm{cm}^{-1}$. This corresponds to matrix element values about 6 ± 2 for the near-resonance interactions of concern (i.e., $v'_V=14\leftrightarrow v'_F=7,8$ and $v'_V=18\leftrightarrow v'_F=5,6$). Notice that the negative curvature observed for $v'=14$, $J'+1/2>4.5$ [Fig. 4(c)] is not reproduced by assuming near-resonance interaction to occur. It could be explained as being largely due to the effect of the stronger off-resonance interaction with $v'=1$ of the E state.

D. Resonance excitation mechanism

It has been shown for HBr that the intensity ratio of the O and S line series to the Q line series ($I(O,S)/I(Q)$) for the $E\leftarrow X$ (2+1)REMPI spectra drop with v'.[27] Based on the dependence of REMPI line intensities on one-photon transition moments for transitions to and from virtual intermediate states[36] it has been concluded that this observation can be due to a gradual change in contributions of parallel ($\mu_\parallel$) versus perpendicular ($\mu_\pm$) transitions moments. An inspection of the $I(O,S)/I(Q)$) ratio for the $V\leftarrow X$ transition for HCl has shown the following trend with energy/v': The $I(O,S)/I(Q)$ ratio was about constant for $v'=8-12$, after which it gradually dropped to $v'=20$ and stayed approximately constant after that up to $v'=26$. As described in Ref. 27 the $I(O,S)/I(Q)$ ratio can be correlated with a ratio of

two parameters, μ_I^2 and μ_S^2(i.e., μ_I^2/μ_S^2), via simulation calculations. For $\Omega=0$ to $\Omega=0$ transition μ_I^2 and μ_S^2 are defined as

$$\mu_S^2=|2\mu_\parallel\mu_\parallel'-\mu_+\mu_-'|^2, \tag{12}$$

$$\mu_I^2=|\mu_\parallel\mu_\parallel'+\mu_+\mu_-'|^2, \tag{13}$$

where the undashed transition moments refer to possible transitions from the ground state to the virtual intermediate state and the dashed ones refer to possible transitions from the virtual states to the resonance excited state.[27] Correlation analysis revealed the following: (i) The ratio (μ_I^2/μ_S^2) is about 0.25 for $v'=8-12$, (ii) it increases to about 0.9 up to $v'=20$, (iii) after which it is found to be essentially unchanged up to $v'=26$. Based on Eqs. (11) and (12) this ratio is 0.25 for purely parallel transitions ($\mu_\pm=0;\ \Omega=0$ intermediate state) but 1.0 for purely perpendicular transitions ($\mu_\parallel=0;\ \Omega=1$ intermediate state). Although these ratio values could be obtained by other combinations of transition moment values, this could mean that a gradual increase in perpendicular transitions/decrease in parallel transitions is occurring as v' increases from $v'=12$ to $v'=20$. The most likely virtual states to contribute significantly to the double perpendicular transition step would be the repulsive Π states $A\,^1\Pi$ and $a\,^3\Pi_i$. The double parallel transition could be represented by

$$V([\sigma\pi^4]\sigma^*)\leftarrow[\sigma\pi^4]\sigma\leftarrow X[\sigma^2\pi^4],$$

where $[\sigma\pi^4]\sigma$ is representative of all virtual Rydberg states with σ Rydberg electron configurations. The double perpendicular transition could be

$$V([\sigma\pi^4]\sigma^*)\leftarrow[\sigma^2\pi^3]\sigma^*\leftarrow X[\sigma^2\pi^4].$$

IV. CONCLUSIONS

Rotational structure of room temperature (2+1) REMPI spectra of HCl and HBr corresponding to the electronic transitions $F\leftarrow X$, $E\leftarrow X$, and $V\rightarrow X$ have been analyzed and interpreted. A large number of vibrational bands has been simulated and/or used to derive rotational level energies in the excited states. Vibrational and rotational spectroscopic parameters derived for the F states from the simulation analyses compare nicely with earlier work made by conventional analysis techniques.[15,21] A high level of consistency was found in level energies and spacings between levels derived from different rotational line series.

Near-resonance interactions between the V states and the F states were evident from analysis of the data for both states, for (i) HCl, $v_F'=1$ and $v_V'=14$, (ii) HBr, $v_F'=1$ and $v_V'=m+7$ and (iii) HCl, $v_F'=2$ and $v_V'=18$. The effects were either seen as shifts of rotational lines relative to calculated line positions or as irregularities in level energy spacings. Off-resonance interactions between the E and the V states were evident by characteristic curvatures observed in plots of level spacings as functions of rotational quantum numbers. Positive curvature occurs in plots of level spacings for the V state when the major perturbing E state is lower in energy, while a negative curvature is obtained for interaction from higher energy perturbing states. Model calculations based on perturbation theory were performed and successfully interpreted the data plots of the level energy spacings, both in terms of near- and off-resonance interactions. Qualitatively, shapes of ''energy spacing curves'' could be reproduced. Quantitatively, orders of magnitude of interaction strengths could be evaluated for HCl. Interaction strengths between close lying vibrational states in the E and the V states were found to be in the range 200–300 cm^{-1}, while near-resonance interaction strengths between states within F and V are found to be about 5–8 cm^{-1}.

Variations observed in the intensity ratio of O and S line series to Q line series in vibrational bands of the V state for HCl are interpreted in terms of the effect of intermediate states on the two-photon excitation mechanism. The observations are consistent with the gradually increasing importance of perpendicular to parallel transitions with increasing energy.

ACKNOWLEDGMENTS

The financial support of the University Research Fund, University of Iceland, the Icelandic Science Foundation, as well as of the Icelandic Research Fund for Higher Education is gratefully acknowledged.

[1] W. C. Price, Proc. R. Soc. London, Ser. A **167**, 216 (1938).
[2] R. F. Barrow and J. G. Stamper, Proc. R. Soc. London, Ser. A **263**, 259 (1961).
[3] R. F. Barrow and J. G. Stamper, Proc. R. Soc. London, Ser. A **263**, 277 (1961).
[4] S. G. Tilford, M. L. Ginter, and J. T. Vanderslice, J. Mol. Spectrosc. **33**, 505 (1970).
[5] S. G. Tilford and M. L. Ginter, J. Mol. Spectrosc. **40**, 568 (1971).
[6] D. S. Ginter and M. L. Ginter, J. Mol. Spectrosc. **90**, 177 (1981).
[7] S. G. Tilford, M. L. Ginter, and A. M. Bass, J. Mol. Spectrosc. **34**, 327 (1970).
[8] M. L. Ginter, S. G. Tilford, and A. M. Bass, J. Mol. Spectrosc. **57**, 271 (1975).
[9] D. S. Ginter, M. L. Ginter, and S. G. Tilford, J. Mol. Spectrosc. **90**, 152 (1981).
[10] D. S. Ginter, M. L. Ginter, S. G. Tilford, and A. M. Bass, J. Mol. Spectrosc. **92**, 55 (1982).
[11] D. S. Ginter, M. L. Ginter, and S. G. Tilford, J. Mol. Spectrosc. **92**, 40 (1982).
[12] J. B. Nee, M. Suto, and L. C. Lee, J. Chem. Phys. **85**, 719 (1986).
[13] J. B. Nee, M. Suto, and L. C. Lee, J. Chem. Phys. **85**, 4919 (1986).
[14] T. A. Spiglanin, D. W. Chandler, and D. H. Parker, Chem. Phys. Lett. **137**, 414 (1987).
[15] D. S. Green, G. A. Bickel, and S. C. Wallace, J. Mol. Spectrosc. **150**, 303 (1991).
[16] D. S. Green, G. A. Bickel, and S. C. Wallace, J. Mol. Spectrosc. **150**, 354 (1991).
[17] D. S. Green, G. A. Bickel, and S. C. Wallace, J. Mol. Spectrosc. **150**, 388 (1991).
[18] D. S. Green and S. C. Wallace, J. Chem. Phys. **96**, 5857 (1992).
[19] E. de Beer, B. G. Koenders, M. P. Koopmans, and C. A. de Lange, J. Chem. Soc., Faraday Trans. **86**, 2035 (1990).
[20] Y. Xie, P. T. A. Reilly, S. Chilukuri, and R. J. Gordon, J. Chem. Phys. **95**, 854 (1991).
[21] R. Callaghan and R. J. Gordon, J. Chem. Phys. **93**, 4624 (1990).
[22] Á. Logadóttir, M.S. thesis, Iceland, 1997.
[23] Á. Kvaran, H. Wang, and Á. Logadóttir, *Recent Research Developments in Physical Chemistry* (Transworld Research Network, 1998), Vol. 2, pp. 233–244.
[24] S. A. Wright and J. D. McDonald, J. Chem. Phys. **101**, 238 (1994).
[25] S. T. Pratt and M. L. Ginter, J. Chem. Phys. **102**, 1882 (1995).
[26] E. de Beer, W. J. Buma, and C. A. deLange, J. Chem. Phys. **99**, 3252 (1993).

[27] Á. Kvaran, Á. Logadóttir, and H. Wang, J. Chem. Phys. **109**, 5856 (1998).
[28] Á. Kvaran, B. G. Waage, and H. Wang (unpublished).
[29] M. Bettendorff, S. D. Peyerimhoff, and R. J. Buenker, Chem. Phys. **66**, 261 (1982).
[30] S. J. Dixon-Warren, R. C. Jackson, J. C. Polanyi, H. Rieley, J. G. Shaper, and H. Weiss, J. Phys. Chem. **96**, 10983 (1992).
[31] R. C. Jackson, J. C. Polanyi, and P. Sjövall, J. Chem. Phys. **102**, 6308 (1995).
[32] W. Huasheng, J. Ásgeirsson, Á. Kvaran, R. J. Donovan, R. V. Flood, K. P. Lawley, T. Ridley, and A. J. Yencha, J. Mol. Struct. **293**, 217 (1993).
[33] Á. Kvaran, H. Wang, and J. Ásgeirsson, J. Mol. Spectrosc. **163**, 541 (1994).
[34] R. J. Donovan, R. V. Flood, K. P. Lawley, A. J. Yencha, and T. Ridley, Chem. Phys. **164**, 439 (1992).
[35] Á. Kvaran, H. Wang, and G. H. Jóhannesson, J. Phys. Chem. **99**, 4451 (1995).
[36] R. G. Bray and R. M. Hochstrasser, Mol. Phys. **31**, 1199 (1976).
[37] K. P. Hüber and G. Herzberg, *Constants of Diatomic Molecules* (Van Nostrand-Reinhold, New York, 1979).
[38] G. Herzberg, *Molecular Spectra and Molecular Structure: I. Spectra of Diatomic Molecules*, 2nd ed. (Van Nostrand Reinhold, New York, 1950).
[39] H. Lefebvre-Brion and R. W. Field, *Perturbations in the Spectra of Diatomic Molecules* (Academic, London, 1986).
[40] R. Liyanage, R. J. Gordon, and R. W. Field, J. Chem. Phys. **109**, 8374 (1998).